J. Fluid Mech. (1983), *vol.* 135, *pp.* 301–321
Printed in Great Britain

Highly nonlinear short-crested water waves

By A. J. ROBERTS†
Department of Applied Mathematics and Theoretical Physics, Silver St, Cambridge CB3 9EW

(Received 9 December 1982 and in revised form 21 June 1983)

The properties of a fully three-dimensional surface gravity wave, the short-crested wave, are examined. Linearly, a short-crested wave is formed by two wavetrains of equal amplitudes and wavelengths propagating at an angle to each other. Resonant interactions between the fundamental and its harmonics are a major feature of short-crested waves and a major complication to the use at finite wave steepness of the derived perturbation expansion. Nonetheless, estimates are made of the maximum steepnesses, and wave properties are calculated over the range of steepnesses. Although results for values of the parameter θ near 20° remain uncertain, we find that short-crested waves can be up to 60% steeper than the two-dimensional progressive wave. At limits of the parameter range the results compare well with those for known two-dimensional progressive and standing water waves.

1. Introduction

Two-dimensional surface gravity waves have been extensively studied over the past 140 years as being the basic pattern of wave motion that occurs on the sea's surface. Most of the research on finite-amplitude waves has concentrated on steady progressive water waves. Fully three-dimensional surface gravity waves have, because of their inherently higher complexity, received rather less attention. In this paper we investigate perhaps the most simple, non-trivial, three-dimensional surface wave motion, that of short-crested waves.

A short-crested system of waves is defined as being a propagating surface gravity wave that is not only periodic in its direction of propagation but it also periodic in the perpendicular horizontal direction (see figure 1). Linearly, this system is found when two wavetrains with equal wavelengths and amplitudes are propagating at an angle to each other. Thus at one end of the short-crested wave's parameter range there are the two-dimensional progressive waves, while at the other end of the parameter range there are two-dimensional standing waves. Both of these limits have features of interest. The standing-wave limit is briefly discussed in the Appendix, while the progressive wave limit is investigated in the companion paper (Roberts & Peregrine 1983).

Short-crested waves may occur in a number of important maritime situations. Swell being fully reflected off a vertical seawall or jetty results in a short-crested system of waves being found adjacent to the reflecting wall. Waves propagating down a vertical-walled channel can assume a short-crested wave form when there is a cross-channel variation of the flow pattern. The waves may also occur when a wavetrain is diffracted behind an obstacle of finite width. Short-crested waves not only have a more complicated free-surface shape than two-dimensional surface waves (figure 1), but, as will be shown in §5, they can be steeper.

† Present address: Department of Applied Mathematics, University of Adelaide, GPO Box 498, Adelaide, South Australia 5001.

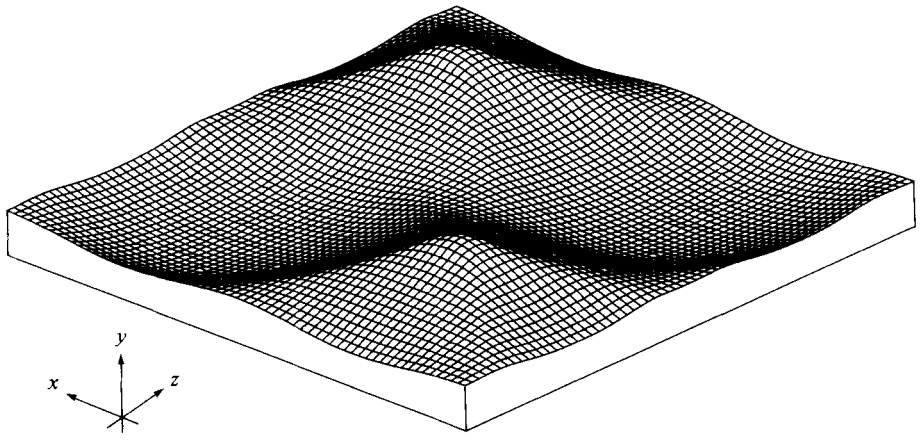

FIGURE 1. Perspective drawing of a one-wavelength rectangle of the short-crested water wave's free surface for $\theta = 45°$ and wave steepness $h = 0.66$. The wave propagates in the x-direction.

In a linear description, the short-crested wave's velocity potential and surface shape are just given by a superposition of the linear progressive surface wave solutions. A second-order solution was obtained by Fuchs (1952), while Chappelear (1961) calculated a third-order perturbation expansion in dimensional form. In order to make easier the calculation of the limit to standing waves, Hsu, Tsuchiya & Silvester (1979) recalculated this third-order expansion in a non-dimensional form using a different perturbation parameter. However, it will be shown in the Appendix that this limit is discontinuous at the fourth order. Roberts (1982) calculated a further third-order expansion with the difference that it is based on a three-dimensional generalization of mapping from the velocity-potential–stream-function space to the physical space. These approximate descriptions of short-crested waves, in particular the third-order expansion of Hsu *et al.* (1979), may be used to estimate some coastal processes. Hsu, Silvester & Tsuchiya (1980) have calculated the sediment transport on the sea floor due to the short-crested waves found near to a reflecting wall, while Fenton (1983) has calculated the pressure forces exerted upon a wall due to the reflection of incident waves.

Numerical schemes can be devised to obtain more accurate descriptions. A numerical calculation of short-crested waves in very shallow water has been described by Bryant (1982), but it is only accurate to $O(a/h)$, where a is the wave amplitude and h is the mean water depth. A method to calculate short-crested waves in water of arbitrary depth has been described in Roberts & Schwartz (1983) and some results are given which are accurate for moderately steep waves in deep water. However, in such numerical solutions it is easy to overlook significant physical processes which occur in the wave, and the numerics often consume an inordinate amount of computer time. The high-order perturbation expansions described in this paper are relatively cheap to compute and significantly extend the obtainable solutions.

In a brief note Mollo-Christensen (1981) has looked at the stability of weakly nonlinear short-crested waves and concluded that some short-crested waves can be stable to modulations purely in the direction of propagation. However, his analysis is deficient because not only does it ignore modulations with a component in the other horizontal direction; but it also uses a theory (described by Whitham 1974) which is only apt for a wavefield describable by a single phase function, whereas short-crested

waves need two phase functions. The dangers in using such methods out of context can be shown through the anomaly incurred by calculating the group velocity of a short-crested wave in a similar manner. He differentiates the leading-order frequency ω_0 with respect to the absolute value of the wavenumber to evaluate the modulational stability criterion $\omega_0''\omega_2 > 0$. However, following the same procedure to derive the group velocity, we would differentiate once to derive the result $\frac{1}{2}(g|k|)^{\frac{1}{2}}/k_1$, where k_1 is the wavenumber in the direction of propagation. As $k_1 \to 0$ with $|k|$ fixed, the 'group velocity' becomes infinite and is clearly wrong. A basic theory for multiphase wavefields (like the short-crested wave) has been developed by Ablowitz & Benny (1970) and Ablowitz (1971, 1972, 1975).

The aim of this paper is to elucidate some of the highly nonlinear properties of steadily propagating short-crested waves. In this initial analysis, unsteady phenomena are not analysed (although they are discussed in §4 in the context of harmonic resonance). The fluid is assumed to be incompressible, inviscid, irrotational and of infinite depth. A high-order perturbation expansion in the wave steepness is derived (§3) and calculated numerically. The occurrence of a doubly infinite family of harmonic resonances are discovered (§4) which cause the perturbation series to have an everywhere zero radius of convergence. However, Roberts (1981) has shown that useful results can still be extracted from a perturbation series which involves harmonic resonance. Estimates are then made of the maximum steepnesses of short-crested waves (§5) and the properties of steep waves.

2. System of equations

We wish to describe a progressive gravity wave with a velocity field and surface shape that is not only periodic in the direction of propagation, but also periodic in the other horizontal direction. The wave is assumed to propagate in the x-direction without change of shape. The y-axis is vertically up and the z-axis is horizontal and completes a right-handed orthogonal system of coordinates.

Let the period of the wave in the x-direction be $L/\sin\theta$ and the period in the z-direction be $L/\cos\theta$. Thus if we were considering the case of an incident wave being fully reflected off a vertical wall, L would be the wavelength of the incident wave, and θ would be the angle between the direction of propagation of the incident wave and the normal to the wall. Hence the limit $\theta \to 90°$ should give the two-dimensional progressive wave, while the limit $\theta \to 0°$ should give the two-dimensional standing wave.

Let the surface shape of the short-crested wave be given by $y = \eta(x, z, t)$. Since the fluid motion is assumed to be incompressible, irrotational and inviscid, we look for a velocity potential $\phi(x, y, z, t)$ that satisfies Laplace's equation in the region $y < \eta(x, z, t)$.

To put all the equations into non-dimensional form, we set $k = 2\pi/L$ and scale all the variables with respect to the reference length $1/k$ and the reference time $(gk)^{-\frac{1}{2}}$. Because of the assumption that the wave is propagating without change of shape we may then solve for the functions $\phi(X, y, Z)$ and $\eta(X, Z)$, periodic in X and Z with period 2π, where

$$X = px - \omega t, \quad Z = qz, \tag{2.1}$$

and where p and q are the non-dimensional x- and z-direction wavenumbers respectively, and are defined by

$$p = \sin\theta, \quad q = \cos\theta. \tag{2.2}$$

For $\theta = 0$ the inherently unsteady standing wave will be described with $X = -\omega t$ being a timelike variable.

Laplace's equation for the velocity potential becomes

$$p^2\phi_{XX} + \phi_{yy} + q^2\phi_{ZZ} = 0 \quad (y < \eta(X, Z)). \tag{2.3}$$

To write down boundary conditions for this equation it is convenient to define the three functions

$$\left.\begin{aligned} U(X,Z) &= \phi_X(X, \eta(X,Z), Z), \\ V(X,Z) &= \phi_y(X, \eta(X,Z), Z), \\ W(X,Z) &= \phi_Z(X, \eta(X,Z), Z), \end{aligned}\right\} \tag{2.4}$$

which are proportional to the components of the fluid velocity at the free surface; the actual x- and z-direction velocities are given by $pU(X,Z)$ and $qW(X,Z)$ respectively, whereas the vertical velocity is just $V(X,Z)$. The kinematic boundary condition that no fluid crosses the free surface is thus

$$-\omega\eta_X + p^2 U\eta_X - V + q^2 W\eta_Z = 0, \tag{2.5}$$

while the condition of constant pressure at the surface is ensured by the transformed Bernoulli equation

$$-\omega U + \eta + \tfrac{1}{2}(p^2U^2 + V^2 + q^2W^2) = 0. \tag{2.6}$$

Infinitely deep in the fluid a necessary condition for no motion is

$$\phi_y \to 0 \quad \text{as} \quad y \to -\infty. \tag{2.7}$$

To measure the amplitude of the wave we use the wave steepness defined by

$$h = \tfrac{1}{2}[\eta(0,0) - \eta(\pi, 0)], \tag{2.8}$$

which is half the non-dimensional peak-to-trough height since the peak of the wave will be fixed at $(X, Z) = (0, 0)$.

We also define quantities which measure how much energy there is in the wave. Let KE (PE) be the non-dimensional mean kinetic (potential) energy density per unit area in the (x, z)-plane. In terms of the velocity potential and surface shape functions these energy densities can be written as

$$\left.\begin{aligned} \mathrm{KE} &= \frac{\omega}{8\pi^2}\int_0^{2\pi}\int_0^{2\pi} \eta[U + \eta_X V]\,\mathrm{d}X\,\mathrm{d}Z, \\ \mathrm{PE} &= \frac{1}{8\pi^2}\int_0^{2\pi}\int_0^{2\pi} \eta^2\,\mathrm{d}X\,\mathrm{d}Z \end{aligned}\right\} \tag{2.9}$$

(for the derivation of these formulae see Roberts & Schwartz 1983).

3. The perturbation expansion

High-order perturbation expansions have been used extensively to obtain solutions in many free surface-wave problems (Schwartz 1974; Cokelet 1977; Holyer 1980; Schwartz & Whitney 1981; Rottman 1982). We try for a solution to the governing equations (2.3) and (2.5)–(2.7) of the form

$$\left.\begin{aligned} \phi &= \sum_{r=1}^{\infty} h^r \phi_r(X, y, Z), & U &= \sum_{r=1}^{\infty} h^r U_r(X, Z), \\ \eta &= \sum_{r=1}^{\infty} h^r \eta_r(X, Z), & V &= \sum_{r=1}^{\infty} h^r V_r(X, Z), \\ \omega &= \sum_{r=0}^{\infty} h^r \omega_r, & W &= \sum_{r=1}^{\infty} h^r W_r(X, Z), \end{aligned}\right\} \tag{3.1}$$

where U, V and W are defined in terms of ϕ and η by (2.4). The expansion for other perturbation parameters, say ϵ, can easily be found by reverting the series for $\epsilon(h)$ and then substituting the resulting series for $h(\epsilon)$ into the expansion.

After substituting (3.1) into the equations and grouping like powers of h, we get an infinite system of equations which can be solved in succession for all the unknown functions. The equations are of the form

$$\left.\begin{aligned} p^2\phi_{rXX}+\phi_{ryy}+q^2\phi_{rZZ} &= 0,\\ \phi_{ry}\to 0 \quad \text{as} \quad y\to-\infty,&\\ \omega_0\eta_{rX}+V_r &= A_r\\ -\omega_0 U_r+\eta_r &= B_r, \end{aligned}\right\} \quad (r=1,2,3,\ldots) \tag{3.2}$$

$$\left.\begin{aligned} A_r &= \sum_{s=1}^{r-1}[-\omega_{r-s}\eta_{sX}+p^2U_{r-s}\eta_{sX}+q^2W_{r-s}\eta_{sZ}],\\ B_r &= \sum_{s=1}^{r-1}[\omega_{r-s}U_s-\tfrac{1}{2}(p^2U_{r-s}U_s+V_{r-s}V_s+q^2W_{r-s}W_s)]. \end{aligned}\right\} \tag{3.3}$$

So far we have passed over the major complication that U, V and W and hence the U_r, V_r and W_r have a complicated dependence on the ϕ_r and η_r. It is possible to find this dependence by expanding ϕ_X, ϕ_y and ϕ_Z in a Taylor series in y about $y=0$ and then substituting the series of η for y. However, this is by no means an easy task, nor is it necessarily an efficient algorithm. To do better we have to know more about the y-dependence of the functions ϕ_r. The solution of the linear problem and the requirement that the solutions are periodic in both X and Z will suffice to give the general form of the y dependence.

At first order $U_1(X,Z)=\phi_X(X,0,Z)$ and $V_1(X,Z)=\phi_y(X,0,Z)$, thus the linear problem is

$$\left.\begin{aligned} p^2\phi_{1XX}+\phi_{1yy}+q^2\phi_{1ZZ} &= 0,\\ \phi_{1y}\to 0 \quad \text{as} \quad y\to-\infty,&\\ \omega_0\eta_{1X}+\phi_{1y} &= 0 \quad (y=0),\\ -\omega_0\phi_{1X}+\eta_1 &= 0 \quad (y=0), \end{aligned}\right\} \tag{3.4}$$

which has the basic, non-trivial, doubly periodic solution

$$\left.\begin{aligned} \omega_0 &= 1,\\ \eta_1 &= \cos(X)\cos(Z),\\ \phi_1 &= \sin(X)\cos(Z)\exp(y), \end{aligned}\right\} \tag{3.5}$$

where the arbitrary phase of the wave has been fixed so that the peak of the wave is at $(X,Z)=(0,0)$. This form for the linear solution restricts the higher order η_r to be of the form of a sum of $\cos(mX)\cos(nZ)$ and the ϕ_r to be of the form of a sum of $\sin(mX)\cos(nZ)\exp(\alpha_{mn}y)$, where α_{mn} is defined by

$$\alpha_{mn}^2=(pm)^2+(qn)^2. \tag{3.6}$$

Since the y-dependence of ϕ_r involves $\exp(\alpha y)$, for different values of α, the determination of U, V and W from the ϕ_r and η_r will involve the calculation of $\exp[\alpha\eta(X,Z)]$ as a Taylor series in h. Define the functions $E_r(X,Z;\alpha)$ so that

$$\sum_{r=0}^{\infty}h^rE_r(X,Z;\alpha)=\exp[\alpha\eta(X,Z)];$$

then we find that

$$E_0 = 1, \quad E_r = \frac{\alpha}{r} \sum_{s=1}^{r} s\eta_s E_{r-s} \tag{3.7}$$

is an efficient method for calculating the E_r. Also note that E_r is a polynomial in α of degree r; thus a computer program to calculate the perturbation series need not store different expansions of $\exp[\alpha\eta]$ for the different possible α.

Supposing that the general form for the ϕ_r will be

$$\phi_r = \sum_{m,n} b_{rmn} \sin(mX) \cos(nZ) \exp[\alpha_{mn} y];$$

then the first equation of (2.4) becomes

$$U = \sum_{r=1}^{\infty} \left[h^r \sum_{m,n} \sum_{s=1}^{r} m b_{smn} \cos(mX) \cos(nZ) E_{r-s}(X, Z; \alpha_{mn}) \right]. \tag{3.8}$$

Similarly for V and W; thus we find

$$\left.\begin{aligned} U_r &= \phi_{rX}(X, 0, Z) + \bar{U}_r, \\ V_r &= \phi_{ry}(X, 0, Z) + \bar{V}_r, \\ W_r &= \phi_{rZ}(X, 0, Z) + \bar{W}_r, \end{aligned}\right\} \tag{3.9}$$

where

$$\left.\begin{aligned} \bar{U}_r &= \sum_{m,n} \sum_{s=1}^{r-1} m b_{smn} \cos(mX) \cos(nZ) E_{r-s}(X, Z; \alpha_{mn}), \\ \bar{V}_r &= \sum_{m,n} \sum_{s=1}^{r-1} \alpha_{mn} b_{smn} \sin(mX) \cos(nZ) E_{r-s}(X, Z; \alpha_{mn}), \\ \bar{W}_r &= -\sum_{m,n} \sum_{s=1}^{r-1} n b_{smn} \sin(mX) \sin(nZ) E_{r-s}(X, Z; \alpha_{mn}). \end{aligned}\right\} \tag{3.10}$$

$\bar{U}_r$, $\bar{V}_r$ and $\bar{W}_r$ do not involve any dependence on η_r or ϕ_r, hence the dependence of U_r, V_r and W_r upon the rth-order quantities is explicitly given in (3.9).

After substituting (3.9), the boundary conditions as given by the last two equations in (3.2) can be combined to give one boundary condition for ϕ_r which does not involve η_r, it is

$$\phi_{rXX} + \phi_{ry} = A_r - \bar{V}_r - B_{rX} - \bar{U}_{rX} \quad (y = 0), \tag{3.11}$$

where use has been made of $\omega_0 = 1$. In general the right-hand side of (3.11) will contain a term of the form $\sin(X)\cos(Z)$; such a term forces a secular term into the expression for ϕ_r. Secular terms are unallowable as they cause a non-uniform convergence in the (X, Z)-space. Fortunately, the right-hand side of (3.11) also contains the term $2\omega_{r-1}\sin(X)\cos(Z)$, where the value of ω_{r-1} has not yet been determined. Thus at the rth order we choose ω_{r-1} so that the right-hand side of (3.11) has no component of $\sin(X)\cos(Z)$. Also, since $\sin(X)\cos(Z)\exp(y)$ is a homogeneous solution of the differential equation and boundary condition, a multiple of it may be introduced into ϕ_r. The definition of the perturbation parameter will give the necessary multiple. η_r can then be found from the last equation in (3.2) (the mean water level will be identically zero; but, for this to be true in a finite-depth calculation, a constant has to be introduced into (2.6)).

The calculations to solve these equations were programmed first in PASCAL on a CYBER 173 and then translated and improved to FORTRAN on an IBM 370/165. The reason for initially using PASCAL is that the program and subroutines could be written

and the algorithm tested far more simply and easily in PASCAL than in FORTRAN. The FORTRAN version was then written to conserve computer store and central-processer time so that much higher orders could be calculated. If N is the highest order to be calculated then the final version of the program uses computer store like N^4 and computer time like N^7. This compares very favourably with the truncated Fourier-series method of solution (see Roberts & Schwartz 1983), especially as the numerical coefficients on the amount of computer resources used are smaller in magnitude for this method. Double-precision coefficients could be calculated up to the 27th order (the order used in all subsequent calculations) on the IBM in just over two minutes computer time. The coefficients calculated for various angles θ agreed with the infinite-depth limit of the third-order expansion given by Hsu *et al.* (1979) and also agreed with the behaviour of the coefficients given by the truncated Fourier series as the steepness was varied. The agreement between these three independent methods would indicate that all three are producing their correct answer. Agreement was also found with Chappelear's (1961) infinite-depth limit, except for one of his coefficients, which differs by a factor of two.

4. Harmonic resonance

For a number of different angles θ a division by zero occurs at some orders in the calculation of the perturbation expansion. Near these critical angles the radius of convergence is very small due to the division by a number which is nearly zero, causing the coefficients at higher orders in the perturbation series to increase rapidly. The divisions by zero occur at these critical angles because one of the harmonics of the linear solution, $\sin(mX)\cos(nZ)\exp(\alpha_{mn}y)$ say, is a homogeneous solution of the linear differential equation. At the $\max(m,n)$th and higher orders, nonlinear combinations of the lower orders usually introduce a non-zero component of this homogeneous solution into the forcing terms on the right-hand side of (3.11), and so we get an unacceptable secular term in the solution for ϕ_r and thus also for η_r. This phenomenon is called harmonic resonance because the fundamental, through the nonlinear coupling, resonantly excites any harmonic which travels at the same phase speed.

The angles at which harmonic resonance occurs in short-crested waves can be calculated by finding the angle θ_c at which any given term is a homogeneous solution of the linear differential equation. We find that the expansion will become secular with respect to the term $\sin(mX)\cos(nZ)\exp(\alpha_{mn}y)$ at

$$\cos^2\theta_c = \frac{m^4-m^2}{n^2-m^2}. \tag{4.1}$$

Listed in table 1 is this doubly infinite family of critical angles. When $n = m^2$ we find $\theta = 0$ for all m; these harmonic resonances correspond to the more familiar resonances that occur in standing gravity waves (see the Appendix). If $m = 1$ then $\theta = 90°$ for all $n > 1$, the reasons for this family of resonances are discussed in Roberts & Peregrine (1983).

When m is odd and n is even, or *vice versa*, the forcing of the (m,n)th harmonic is always zero (because of the wave's triangular symmetry) and hence these entries are missing from this table of harmonic resonances. However, these solutions of (4.1) give the locations of those bifurcations which occur at an infinitesimal amplitude and which involve the introduction of a harmonic of the fundamental wave (3.5). Since both resonances and bifurcations are described by (4.1) we see that they are, in some

n	$m=1$	$m=2$	$m=3$	$m=4$	$m=5$
3	90.0000°				
4		0.0000°			
5	90.0000°				
6		52.2388°			
7	90.0000°				
8		63.4349°			
9	90.0000°		0.0000°		
10		69.2952°			
11	90.0000°		36.6992°		
12		72.9761°			
13	90.0000°		47.8696°		
14		75.5225°			
15	90.0000°		54.7356°		
16		77.3956°		0.0000°	
17	90.0000°		59.5296°		
18		78.8342°		28.0260°	
19	90.0000°		63.1108°		
20		79.9750°		37.7612°	
21	90.0000°		65.9052°		
22		80.9026°		44.2654°	
23	90.0000°		68.1546°		
24		81.6719°		49.1066°	
25	90.0000°		70.0084°		0.0000°
26		82.3206°		52.9133°	
27	90.0000°		71.5651°		22.6046°

TABLE 1. Angles θ_c at which harmonic resonance occurs with the (m,n)th harmonic in an infinite-depth fluid

sense, similar phenomena; this connection has also been pointed out by Chen & Saffman (1979).

In finite depth (4.1) no longer holds. Instead the correct equation relating the angle θ and the depth d to the (m,n)th harmonic with which resonance may occur and zero divisors appear in the perturbation expansion is given by

$$\alpha_{mn}\tanh(\alpha_{mn}d) = m^2\tanh(d), \tag{4.2}$$

(see table 2 for a typical set of solutions of this equation). In the equation the implicit dependence on θ and n is in the definition of α_{mn} given by (3.6). Equation (4.2) reduces to (4.1) in the infinite-depth limit, and as $\theta\to 0$ it reduces to the condition given by Tadjbakhsh & Keller (1960) for uniqueness of their solution for standing gravity waves in a finite-depth fluid. Equation (4.2) thus corrects the uniqueness condition for short-crested waves that Hsu *et al.* (1979) presented in their equation (19).

The structures displayed in tables 1 and 2 are very similar – in particular they both have the infinite number of resonances at the limit to the two-dimensional progressive wave $\theta = 90°$. Also, these critical angles are everywhere dense on the θ-interval $[0°, 90°]$; that is, there is a critical angle arbitrarily close to every angle between 0° and 90°. Since the radius of convergence is zero at these θ_c it follows that the perturbation series has an everywhere zero radius of convergence! This is similar to the conclusion that Concus (1964) reached for standing capillary–gravity waves.

In many wave problems harmonic resonance occurs at a family of isolated

n	$m=1$	$m=2$	$m=3$	$m=4$	$m=5$	$m=6$	$m=7$
3	90.0000°						
4		71.8333°					
5	90.0000°		40.3734°				
6		78.9931°					
7	90.0000°		61.1950°				
8		81.9849°		25.9592°			
9	90.0000°		68.9529°				
10		83.6713°		47.1829°			
11	90.0000°		73.2648°				
12		84.7627°		56.5926°			
13	90.0000°		76.0595°		29.7811°		
14		85.5295°		62.3353°			
15	90.0000°		78.0331°		42.5691°		
16		86.0988°		66.2909°			
17	90.0000°		79.5051°		50.1330°		
18		86.5386°		69.2102°		23.8903°	
19	90.0000°		80.6523°		55.3757°		
20		86.8888°		71.4651°		35.5815°	
21	90.0000°		81.5691°		59.2932°		
22		87.1743°		73.2651°		42.8540°	
23	90.0000°		82.3203°		62.3592°		10.6062°
24		87.4117°		74.7381°		48.1082°	
25	90.0000°		82.9473°		64.8369°		26.1978°
26		87.6122°		75.9676°		52.1682°	
27	90.0000°		83.4789°		66.8876°		34.3289°

TABLE 2. Angles θ_c at which harmonic resonance occurs with the (m, n)th harmonic in water of non-dimensional depth $d = \frac{1}{2}$

resonances (e.g. capillary–gravity waves). Roberts (1981), in a study of a model wave equation, predicts that in general there are three distinct solutions in a region about the convergence limiting (pole) singularity associated with each resonance (see figure 2 for the typical behaviour near harmonic resonance or see figures 12 and 13 in Roberts (1981) or figure 8 in Chen & Saffman (1979)). Further, convergence acceleration techniques, like the Padé approximants or the Shanks transform, applied to an amplitude expansion converge to a solution for amplitudes up to and past the singularity. For high harmonic resonances the triple solution structure is very localized, and the largest error incurred by truncating the expansion at an order N, and so ignoring any resonances of higher order, is $O(h_3^{\frac{1}{3}N})$. Hence the converged answers correspond to a solution of the equations with some error, the error can be made small by increasing N.

An equivalent analysis to that of Roberts (1981) shows that precisely the predicted qualitative structures occur for each of the (2, 6) and (2, 8) harmonic resonances in short-crested waves (figure 2). We assume that the predictions hold for all the harmonic resonances in short-crested waves except possibly those occurring for $\theta = 0°$ and $\theta = 90°$. Although the resonances are dense over θ we realize that almost all of the resonances are of very high order. These very-high-order resonances contribute an exceedingly fine structure to the solutions and the error incurred by truncating the expansion at finite N and ignoring such detail is small, the error being at most of order $h_3^{\frac{1}{3}N}$.

However, we want to use the perturbation series to calculate such quantities as

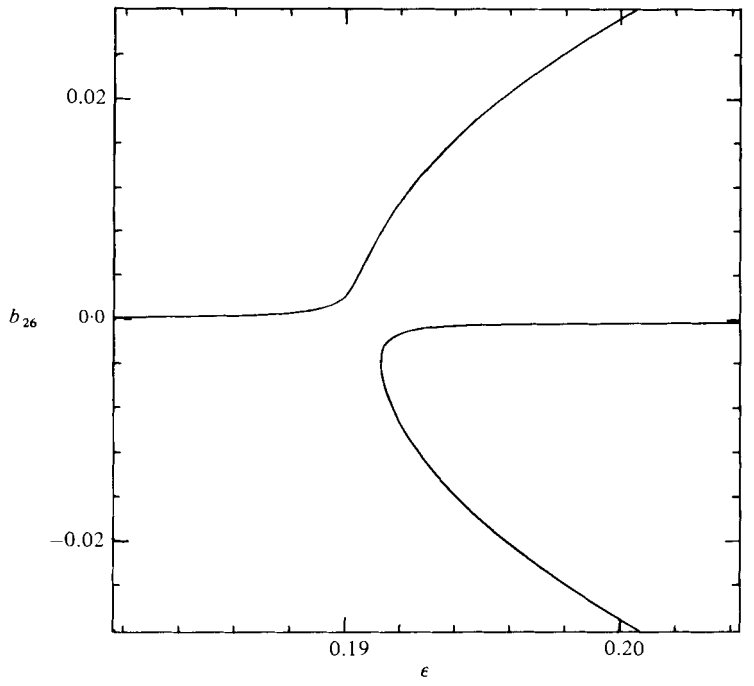

FIGURE 2. The typical structure of a wave solution near any one harmonic resonance, here the (2, 6) harmonic resonance of short-crested waves. The value of b_{26}, the coefficient of the $\sin(2X)\cos(6Z)\exp(\alpha_{26}y)$ component in the velocity potential, is plotted against ϵ, the coefficient of the $\sin(X)\cos(Z)\exp(y)$ component in the velocity potential, for fixed $\theta = 53°$. The formula from which the curve is plotted was derived from a sixth-order perturbation expansion in ϵ based at $\theta = 52.2388°$ (for more details see Roberts 1981, 1982).

the maximum steepness of a short-crested wave; realizing that in the presence of so many possible solutions due to the harmonic resonances such quantities may not be well defined. In a Taylor's series of an analytic function the behaviour of the coefficients is ultimately dominated by the nature and location of the singularity that is nearest to the centre of expansion. But, if the nearest singularity is a weak one and if there is a stronger singularity further away, then a finite number of consecutive coefficients may have their values dominated by the nature and location of the more distant singularity. Thus if the close singularities are weak then a numerically obtained Taylor's series may contain a large amount of information about distant singularities and hence about the distant behaviour of the function. In short-crested waves most of the singularities due to the harmonic resonances are extremely weak, in fact almost all of the singularities are so weak that they do not affect the coefficients of a finite truncation of the perturbation series in any way. Moreover, all the harmonic resonance singularities which were detected in the perturbation expansion are simple poles (except for the $m = 1$, $n > 1$ resonances for which the associated singularities lie off the real h-axis). Hence the short-crested wave solution is real-valued for real h past the singularity. Thus it is physically meaningful to talk about and obtain solutions with a larger amplitude.

These arguments are strikingly confirmed in the Appendix, where the limit of the perturbation expansion as θ tends to 0° can be compared with known expansions for the two-dimensional standing wave. In this limit we calculate the expansion

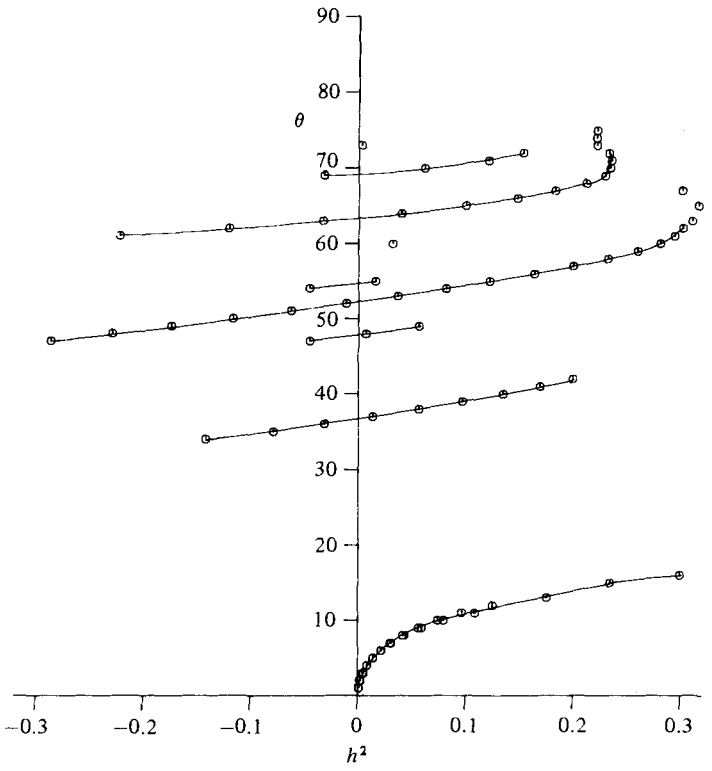

FIGURE 3. Locations of harmonic resonance in short-crested waves. The data points (circles) are the locations of those poles common to both the [6, 6] and [6, 7] Padé approximants of the frequency expansion (calculated at 1° intervals); the lines interpolate between the data and are purely for visualization. The poles at positive h^2 correspond to physical jumps between one possible solution and another due to harmonic resonance. The resonances shown can be recognized as the standing-wave resonance and then as θ increases, the (3, 11), (3, 13), (2, 6), (3, 15), (3, 17), (2, 8), (2, 10) and (2, 12) resonances.

corresponding to the form of the solutions past the pole singularities of the standing-wave resonances. To numerical error the resulting coefficients agree with those given by Schwartz & Whitney (1981).

The harmonic resonances that are strong enough to affect significantly the 27th-order perturbation expansion of short-crested waves can be discerned in figure 3, in which are plotted the locations of the poles, attributable to harmonic resonances, of the [6, 7] Padé approximant of the frequency expansion. This shows the lines in the parameter (h, θ)-plane across which we may expect the wave properties of the presently calculated solutions to undergo a jump from those of one solution branch to those of a different branch.

In the presence of so many solutions due to harmonic resonances, how physically relevant are the steady solutions which we will describe? We have seen that harmonic resonance is much like bifurcation: as such we presume their relevance is similar. Yet discussions of the main solution branch of wave problems have largely ignored its relevance in the presence of indefinitely many undetected bifurcations (Meiron, Saffman & Yuen (1982) make a similar point in their §6). Similarly, numerical solutions of wave problems involving harmonic resonance have largely ignored the resonances; this is possibly because of the extremely restricted region in which any

one resonance is effective. It is the drastic effect that harmonic resonance has upon a perturbation expansion which forces us to address the question here. However, the question is incomplete and we should discuss the relevance of solutions in the presence of bifurcations as well as harmonic resonances.

The resolution of the above question must lie in the behaviour of unsteady solutions to the original equations. Steadily propagating wave solutions can be interpreted as a stationary point in some vast solution space, while unsteady solutions evolve in time along some trajectory in the solution space. The behaviour of unsteady solutions near second and third harmonic resonance can be analysed via the method of multiple scales (McGoldrick 1970, 1972; Nayfeh 1971). The generic behaviour would appear to be that the trajectories in the solution space are closed (though this needs more study); that is, there is a partial and periodic exchange of energy between the fundamental and the resonating harmonic over a long timescale (see e.g. figure 1 of McGoldrick 1970). (It should be noted that these analyses only allow the fundamental and the resonant harmonic to interact – more general unsteady behaviour is excluded by the assumed form of the solution.) A similar type of analysis should be possible to determine the behaviour of solutions near a bifurcation, although the analysis is likely to be more difficult because non-trivial bifurcations typically occur at finite amplitudes. We would expect similar forms for the interaction equations with qualitatively similar solutions.

Thus the relevance of steadily propagating wave solutions depends largely upon the nature of the interaction equations near their stationary points. It will depend upon the stability of the stationary point and, perhaps just as importantly, upon whether the evolution of the wave takes place slowly or relatively quickly near the stationary point. It would appear that analyses of the general types of interactions is needed before the question on the relevance of steady solutions can be answered properly.

5. Steep short-crested waves

The short-crested wave perturbation expansion will contain information about the singularities which occur because of physical limitations on the maximum steepness of the wave, though in finite-precision arithmetic the proximity of lower-order harmonic resonances can severely degrade this information. Maximum amplitudes of short-crested waves are estimated by inspecting the real poles and zeros of the $[M, M]$ and $[M, M+1]$ Padé approximants of the series in h for some of the properties of the wave.

These Padé approximants were calculated via the continued-fraction representation of the series. The continued fraction of a given series truncated at the Nth order can be calculated in order-N^2 operations. From this representation all the $[M, M]$ and $[M, M+1]$ Padé approximants can be calculated successively for a given h using a total of order-N^2 operations. Also the polynomial coefficients of all the numerators and denominators of these Padé approximants can be calculated successively in a total of order-N^2 operations; thus making it a very efficient method – see Bender & Orszag (1978) for details.

The series to which this was applied were those of $\eta_{XX}(0,0)$ and $\eta_{ZZ}(0,0)$, which are proportional to the reciprocal of the x- and z-direction radii of curvature at the wave's peak if h is positive, or at the trough if h is negative. These were used because the singularity limiting the maximum amplitude of a short-crested wave is expected to be due to the formation of a conelike structure at the peak of the wave in some

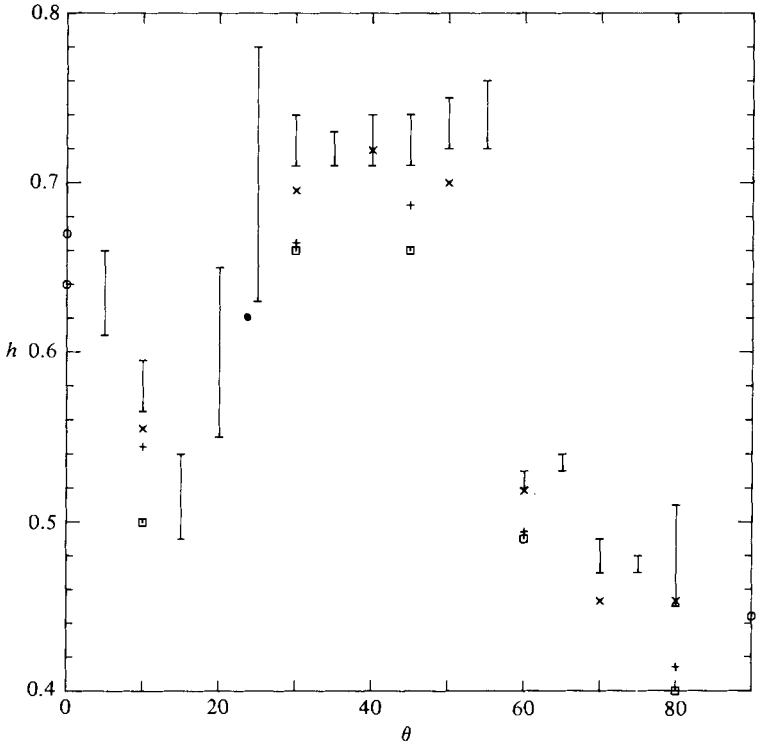

FIGURE 4. Estimates (with rough error bars) of the maximum amplitudes of short-crested waves for different values of θ. Also plotted are: ○, maximum amplitudes of the 2-dimensional progressive and standing waves; ×, steepnesses to which frequencies are plotted in figure 5; +, steepnesses to which energy densities are plotted in figure 6; □, steepnesses at which the free surfaces are drawn in figures 1 and 7.

generalization of Stokes' (1880) limiting corner flow for two-dimensional waves. The real poles and zeros of the Padé approximants occurred in a number of different situations. A pole–zero pair could occur extremely close to each other; typically their separation was less than 10^{-7}. These were not in general consistent from one Padé approximate to another, and were taken to be physically meaningless quirks of some particular Padé approximants. Pole–zero pairs also occurred close together owing to the weak harmonic-resonance singularities, typical separation being around 10^{-4}–10^{-5}, with the larger separations occurring with increasing amplitude at which the resonances are located. These pole–zero pairs were extremely consistent in the Padé approximants once a high-enough order from the series had been used (see figure 3 for the locations at which these occurred). The small separation shows just how weak the resonant structures actually are. Of the remaining poles the smallest positive persistent pole was taken to be an estimate of the maximum wave steepness, although occasional notice was taken of complex conjugate pairs of poles lying near the real h-axis (in particular this was necessary near the troublesome angle $\theta = 20°$).

The estimates of the maximum wave amplitudes obtained in this manner are plotted in figure 4, the bars are an approximate measure of the amount of spread in the location of these poles. Because the Padé approximants put the poles just past the singularity when they represent a simple function, e.g. $(1-h)^{-\frac{1}{2}}$, a true maximum amplitude will be near the bottom of the bars shown. The agreement between the

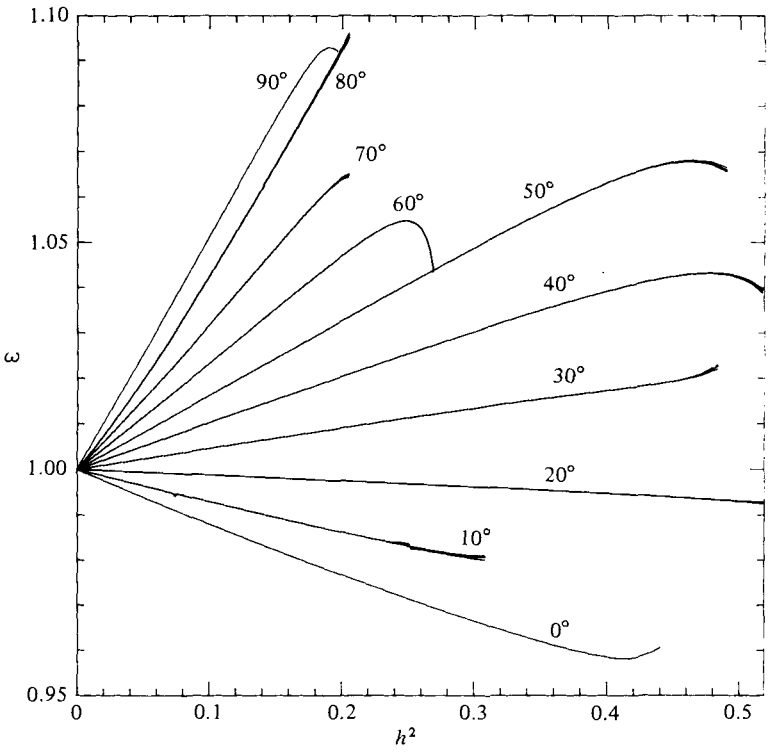

FIGURE 5. Frequency of a short-crested wave as a function of the wave steepness squared for fixed values of θ. For each θ, data is plotted until the estimated error reached 0.0005. The $\theta = 0°$ and $\theta = 90°$ curves were drawn from data taken from Schwartz & Whitney (1981) and Cokelet (1977) respectively.

maximum amplitude estimates for values of θ near 90° and Cokelet's (1977) maximum wave amplitude for two-dimensional progressive waves (indicated by the circle on the right-hand side of figure 4) is reasonable (the near-standing wave results are discussed in the Appendix).

The rapid change in maximum amplitude from the $\theta = 55°$ to 60° shown in figure 4 is due to the different solutions on either side of the (2, 6) harmonic resonance (compare the jump with the location of the (2, 6) harmonic resonance at large amplitudes – see figure 3). A point to note is that it is very hard to distinguish between poles caused by harmonic resonance structures at large amplitudes and those caused by the singularity which limits the amplitude. Across the (2, 6) resonance the (2, 6) harmonic changes sign. On one side of the resonance it will contribute to the peaked shape of the wave in the spanwise (z-) direction, while on the other side it will tend to flatten the spanwise profile. Thus this jump in the maximum possible amplitude is likely to be associated with the transition from the pyramidal surface shape characteristic of midrange values of θ (see figure 1), to the long-crested surface shape characteristic of values of θ near 90° (see figures 7 *c*, *d*).

Estimates of wave properties are obtained using Padé approximants. Graphs are typically drawn from the results of the four [5, 5], [5, 6], [6, 6] and [6, 7] Padé approximants of a 13-term series in h^2 obtained from a 27th-order perturbation expansion. For each property and for each steepness the mean of the four results was taken and then the worst of the four results was thrown away and the remaining three

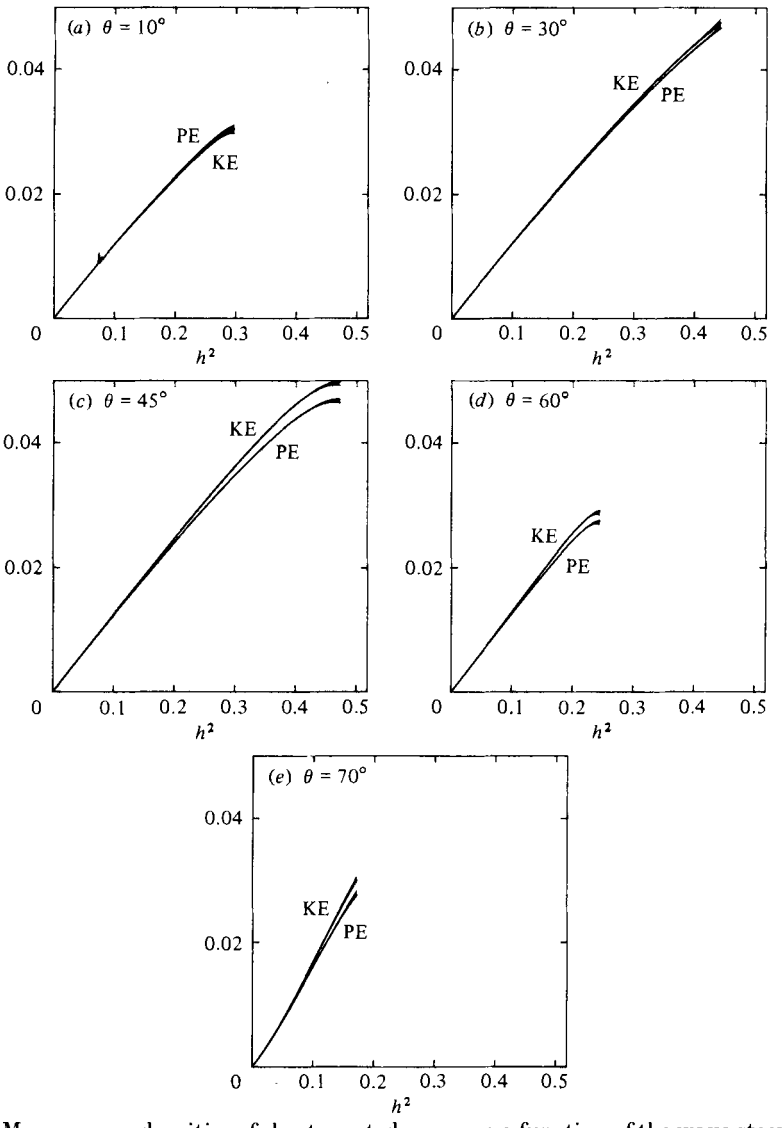

FIGURE 6. Mean energy densities of short-crested waves as a function of the wave steepness squared for selected values of θ. Data is only plotted for heights at which the combined estimated error is less than 0.0005.

results were plotted. This procedure is used to minimize the effects of any independent quirks which may occur in any of the Padé approximants. It may be seen that the curves presented are of graphical accuracy. To obtain more accurate answers at higher wave steepnesses a perturbation expansion calculated with more retained significant digits is likely to be required rather than a higher order of calculation.

Using this estimate of the errors we have also plotted in figure 4 the steepnesses at which calculations of various wave properties have attained a given error, the specified error being independent of θ (the frequency see figure 5, and for the kinetic and potential energies see figure 6). The agreement between this data and the estimated maximum amplitudes is quite good, consistently slightly less than the estimates (except for the $\theta = 20°$ case).

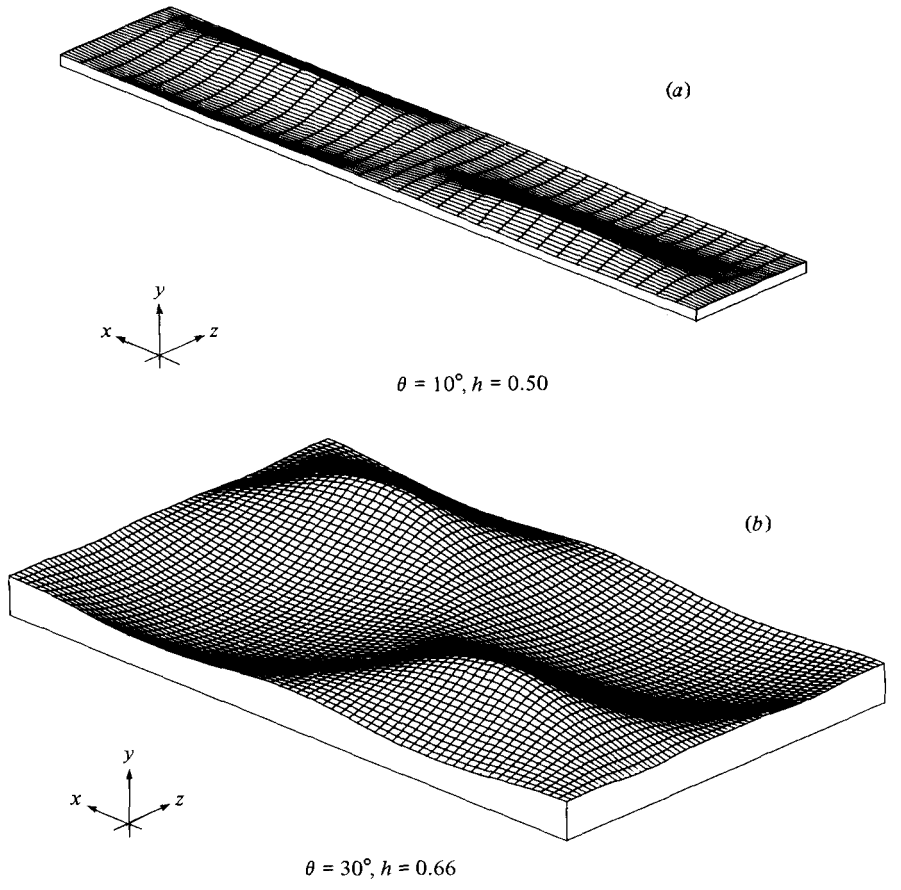

FIGURE 7 (*a*, *b*). For caption see facing page.

In figure 5 are plotted the frequencies ω as a function of the wave steepness for various values of θ, the results for the two-dimensional progressive and standing waves are also drawn for comparison. The criterion for determining the amplitudes at which to stop plotting data was, uniformly across θ, that the estimated error should be less than 0.0005 (an error of $\frac{1}{2}\%$ relative to the maximum frequency variation). We see that for $\theta \gtrsim 40°$ there is, as expected, a maximum in the frequency (and hence in the phase speed) below the maximum wave amplitude. While for $\theta \lesssim 30°$ the opposite effect appears to happen (the frequency of high waves is less than that of the highest wave) which for $\theta \lesssim 20°$ means that a minimum in the wave frequency occurs below the maximum wave amplitude, similar to the case of the two-dimensional standing waves.

The mean kinetic- and potential-energy densities for some short-crested waves are plotted in figure 6. For $\theta > 21.9719°$ the kinetic-energy density is typically larger than the potential-energy density, like the two-dimensional progressive wave. However, for $\theta < 21.9719°$ the potential-energy density is the larger. This critical angle of $\theta = 21.9719°$ is also the angle at which the dispersion relation becomes almost amplitude independent ($\omega_2 = 0$). We also see that for most values of θ there is an energy density maximum, below the maximum amplitude, though this may not be so for θ in roughly the range 20°–30°.

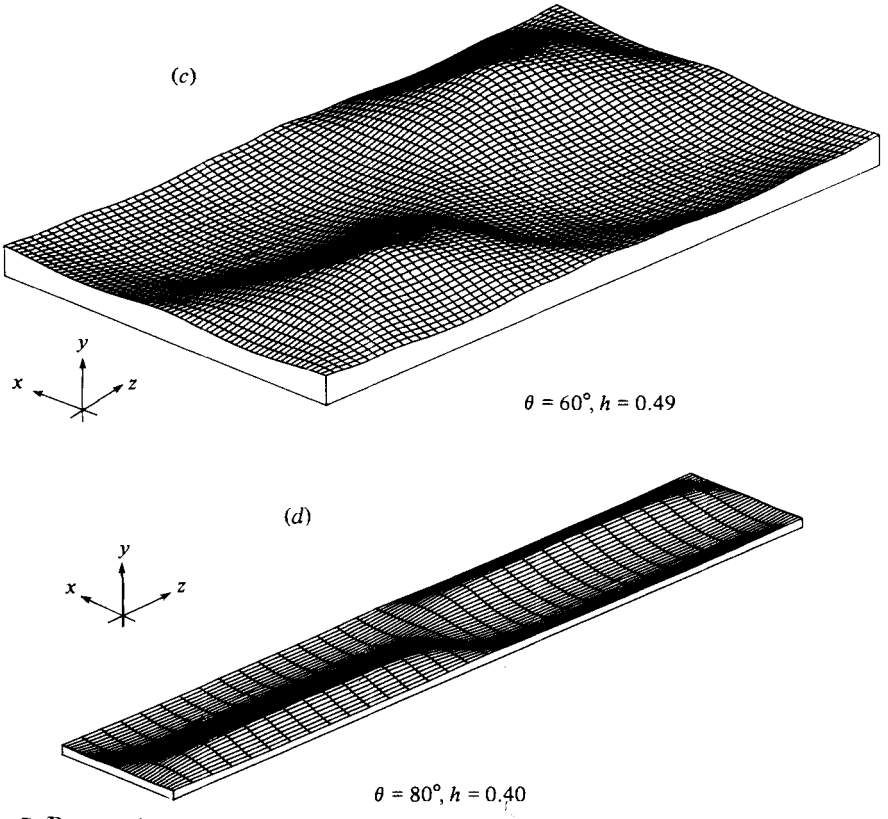

FIGURE 7. Perspective drawings of a one-wavelength rectangle of the free surface for selected values of θ and the wave steepness h.

Representative free surface shapes of high short-crested waves are plotted in figure 1 and in figure 7. The steepnesses for which surfaces could be drawn are plotted on figure 4 for comparison with the other data. We see that the surfaces shown are for waves of about 85–90 % of the maximum wave amplitudes (a figure which is very sensitive to the value taken for the maximum wave amplitude). The shapes of the surfaces vary. The wave is, for θ near 0°, fairly rounded in the direction of propagation and peaked with a relatively flat trough in the z-direction; distinctly pyramidal for values of θ in the middle of the range; for θ near 90° a surface that again has a wide flat trough and a sharp peak, but the crest of the wave is relatively long and flat (discussed further in Roberts & Peregrine 1983).

6. Concluding remarks

Since harmonic resonance plays an important role in any consideration of short-crested waves, the unsteady properties of harmonic resonance are also relevant. It is well established that four intersecting gravity wavetrains can interact and cause long-term amplitude and phase variations in the four component waves. Such third-order resonance with four components does not affect a wavefield composed only of a short-crested wave. However, four intersecting gravity waves can also interact at a higher order, although in this case the variations take place over an even longer timescale. It is such a resonance between the two components of the

fundamental and the two components of some higher harmonic that causes the phenomenon of harmonic resonance in short-crested waves. It is also possible that a general short-crested wave could interact with one of its harmonics to generate a growing short-crested wave component with different periodicities. Thus it seems that the unsteadiness due to the harmonic resonance is important in these waves (discussed in more detail in §4). However, in most physical situations, for example the reflection of swell off a sea wall, the energy travelling in the wave is only in the form of a short-crested wave for a short period of time and so resonance does not have time to become significant. This is fortunate as the unsteady behaviour of harmonic resonances of order higher than third order has so far only been guessed at. Perhaps a more relevant unsteadiness is the edge effects of having a reflection off only a finite length of wall.

Despite the harmonic resonance, 27th-order perturbations have been used to calculate some properties of steady short-crested waves. From the expansions estimates have been made of the maximum wave steepness to within an error of approximately 5%. The data indicates that an upper bound on short-crested wave heights over all the range of the parameter θ is (peak–trough)/(incident wavelength) < 0.24. The analysis also indicates that over a large range of θ the frequencies of short-crested waves have an extremum at steepnesses just lower than the maximum wave amplitude. This is presumably associated with the hypothesis, shown by Longuet-Higgins & Fox (1977) and Cokelet (1977) to be true for two-dimensional progressive waves, that the highest wave is, on average, less extreme than a slightly lower wave. Because the surface is two-dimensional this effect is expected to be more marked for short-crested waves than for progressive waves; the wave speed maximum for progressive waves occurs at an amplitude about 1.6% lower than the maximum amplitude, while for short-crested waves the frequency maximum for $\theta = 45°$ occurs at an amplitude about 10% lower than the maximum amplitude (though this figure is sensitive to the value used for the maximum amplitude and to inaccuracies in the Padé summation). A better choice of the perturbation parameter, perhaps a generalization of the one used by Cokelet (1977), or more precise numerical arithmetic may give more accurate results than those presented here.

Another interesting problem is the form of the solution near the peak of a maximum-amplitude short-crested wave. Stokes (1880) derived the limiting form of the progressive wave's peak, but at the other end of the parameter range the limiting peak shape of the standing wave is still uncertain.

Solutions of the two extremes of the parameter θ are also of interest. In the Appendix the limit to the standing wave is considered. The limit is not continuous and the structure of the solutions near the limit is complicated. A similar scaling to that introduced for the solution of the long-crested waves, being a variation of the wavenumber perturbation technique used by Roberts (1981) should also be able to analyse the near-standing wave structure. The long-crested limit $\theta \to 90°$, discussed in Roberts & Peregrine (1983), describes the properties of the transition between short-crested waves and the well-known two-dimensional progressive waves.

I wish to acknowledge the advice and help of Dr H. E. Huppert and Dr L. W. Schwartz throughout the term of this research, during which I was supported by the Australian Research Council and the Association of Commonwealth Universities.

Appendix. Standing-wave limit

In the limit as θ tends to 0° the short-crested wave system of equations tends to those of the standing gravity wave problem. In this Appendix we consider the behaviour of the perturbation series derived in §3 in this limit and relate it to the known behaviour of standing waves.

Standing gravity waves have been examined by a number of authors. Penney & Price (1952) constructed a fifth-order perturbation expansion in infinite depth. Tadjbakhsh & Keller (1960) extended Penney & Price's results to finite depth and discovered that zero divisors occurred in their expansion at certain depths; these depths they thus prohibited. These zero divisors we now recognize to be symptomatic of the occurrence of harmonic resonance. Penney & Price did not notice this occurrence of harmonic resonance because the forcing of the resonant harmonic is zero up to the fifth order. However, Schwartz & Whitney (1981) showed that Penney & Price's results were incorrect at the fourth order because there was a non-zero forcing of the (2, 4) resonant harmonic $\sin(2t)\cos(4x)$ at the sixth order. Schwartz & Whitney showed that this could be avoided by the correct choice of the (2, 4) harmonic at the fourth order. In general they found that the resonant forcing at the rth order could be avoided by the correct choice of the resonant harmonic at the $(r-2)$th order. They also showed that the same scheme applied to the other resonating harmonics of standing gravity waves in an infinite-depth fluid, i.e. the (3, 9), (4, 16), ... harmonics. Thus they could numerically calculate a high-order perturbation expansion for standing waves and deduce some finite-amplitude results; in particular they estimate that the maximum amplitude of a standing wave lies somewhere between $h = 0.64$ and $h = 0.67$ (see figure 4). In this standing-wave limit the complex structure of short-crested wave solutions and the resultant loss of information in the numerical series coefficients due to the use of finite-precision arithmetic (here 16-digit) cause the large spread in the estimates of the maximum amplitudes. However, the agreement with Schwartz & Whitney's result is fair and indicates that the maximum amplitude of short-crested waves initially falls sharply as θ is increased from zero.

For short-crested waves the standing-wave resonances are indicated in table 1 by the entries $\theta_c = 0.0000°$. It was hoped that the short-crested wave perturbation expansion would tend continuously to a correct convergent standing-wave expansion. However, while the fourth-order coefficient of the (2, 4) harmonic does indeed tend to a finite limit it is the wrong limit. So in the limit the higher-order (2, 4) coefficients are given by a non-zero forcing divided by a zero divisor, which is singular and thus invalidates the lower-order limit. When higher orders are calculated for values of θ near 0 we find that there exists a singularity for real h (figure 3); the location of the singularity occurs at approximately

$$h = \pm[1.22\theta + 1.4\theta^2]. \tag{A 1}$$

Also the type of this singularity is that of a simple pole, characteristics typical of harmonic-resonant perturbation expansions. Because this singularity occurs for real h the limit at finite amplitude from short-crested waves to standing waves is not a continuous one, even though the only harmonic resonances to be considered are the (m, m^2) resonances of the standing wave. The occurrence of the (3, 9) near zero divisor for orders higher than nine appears to cause an extra pole singularity to occur at much the same wave steepness as that given by (A 1). At $\theta = 10°$ we can discern a relatively strong harmonic-resonance structure in figures 5 and 6 near $h^2 = 0.075$. The (4, 16) zero-divisor occurs at too high an order to be sure of its effect or lack thereof.

Because the singularities are poles we expect that the Padé transform would give an answer for real h past the location of the singularities. The two leading diagonals of the Padé table can be calculated from the continued-fraction representation of a Taylor series. For any given component of the short-crested wave we consider the limit of the continued fraction representation at some fixed positive h^2 as $\theta \to 0$. We find that there are two consecutive coefficients in the continued fraction which tend to infinity in such a way that their ratio tends to a finite number. Suppose that the coefficients of the continued fraction in h^2 are given by the sequence (a_r), where the dependence upon the parameter θ is implicit. Further pose that in the continued fraction there exist a pair of coefficients

$$|a_s|, |a_{s+1}| \to \infty \quad \text{as} \quad \theta \to 0 \quad \text{such that} \quad \frac{a_s}{a_{s+1}} \to R \neq -1. \tag{A 2}$$

Then we can show that in the limit as $\theta \to 0$ for fixed h the segment of the continued fraction given by

$$1 + \alpha_{s-1} h^2/(1 + a_s h^2/(1 + a_{s+1} h^2/(1 + a_{s+2} h^2/\mathrm{CF}))), \tag{A 3}$$

where CF represents the higher-order terms of the continued fraction, reduces to the expression

$$1 + \frac{a_{s-1}}{R+1} h^2 \Big/ \left(1 + \frac{R a_{s+2}}{R+1} h^2 \Big/ \mathrm{CF}\right), \tag{A 4}$$

a continued fraction with two fewer coefficients. CF is the same continued-fraction expression as in (A 3). If desired, the modified continued faction obtained in (A 4) may then be reverted back to a Taylor series in h^2.

Applying this to calculated expansions for θ near 0° we find that each of the resonant harmonics contributes a pair of coefficients which tend to infinity in the continued fraction. Thus the above reduction has to be carried out for each of these pairs. After reverting back to a Taylor series we find that the coefficients agree with the coefficients obtained by Schwartz & Whitney (1981) for the standing gravity wave. Thus we see something about the structure of the short-crested wave solutions in this limit and how the solutions relate to the known standing-wave solution of Schwartz & Whitney.

REFERENCES

Ablowitz, M. J. 1971 Applications of slowly varying nonlinear dispersive wave theories. *Stud. Appl. Maths* **50**, 329–344.

Ablowitz, M. J. 1972 Approximate methods for obtaining multi-phase modes in nonlinear dispersive wave problems. *Stud. Appl. Maths* **51**, 17–55.

Ablowitz, M. J. 1975 A note on resonance and nonlinear dispersive waves. *Stud. Appl. Maths* **54**, 61–70.

Ablowitz, M. J. & Benney, D. J. 1970 The evolution of multi-phase modes for nonlinear dispersive waves. *Stud. Appl. Maths* **44**, 225–238.

Bender, C. M. & Orszag, S. A. 1978 *Advanced Mathematical Methods for Scientists and Engineers.* McGraw-Hill.

Bryant, P. J. 1982 Two-dimensional periodic permanent waves in shallow water. *J. Fluid Mech.* **115**, 525–532.

Chappelear, J. E. 1961 On the description of short-crested waves. *Beach Erosion Board, U.S. Army, Corps Engrs, Tech. Memo* no. 125.

Chen, B. & Saffman, P. G. 1979 Steady gravity–capillary waves on deep water – 1. Weakly nonlinear waves. *Stud. Appl. Maths* **60**, 183–210.

COKELET, E. D. 1977 Steep gravity waves in water of arbitrary uniform depth. *Phil. Trans. R. Soc. Lond.* A **286**, 183–230.

CONCUS, P. 1964 Standing capillary gravity waves of finite amplitude: corrigendum. *J. Fluid Mech.* **19**, 264–266.

FENTON, J. D. 1983 Short-crested waves and the wave forces on a wall. Submitted to *J. Waterway, Port, Coastal and Ocean Div. ASCE.*

FUCHS, R. A. 1952 On the theory of short-crested oscillatory waves. *Gravity Waves, U.S. Nat. Bur. Stand. Circular* 521, pp. 187–200.

HOLYER, J. Y. 1980 Large amplitude progressive interfacial waves. *J. Fluid Mech.* **93**, 433–448.

HSU, J. R. C., SILVESTER, R. & TSUCHIYA, Y. 1980 Boundary-layer velocities and mass transport in short-crested waves. *J. Fluid Mech.* **99**, 321–342.

HSU, J. R. C., TSUCHIYA, Y. & SILVESTER, R. 1979 Third-order approximation to short-crested waves. *J. Fluid Mech.* **90,** 179–196.

LONGUET-HIGGINS, M. S. & FOX, M. J. H. 1977 Theory of the almost-highest wave: the inner solution. *J. Fluid Mech.* **80**, 721–742.

MCGOLDRICK, L. F. 1970 On Wilton's ripples: a special case of resonant interactions. *J. Fluid Mech.* **42**, 193–200.

MCGOLDRICK, L. F. 1972 On the rippling of small waves: a harmonic nonlinear nearly resonant interaction. *J. Fluid Mech.* **52**, 725–751.

MEIRON, D. I., SAFFMAN, P. G. & YUEN, H. C. 1982 Calculation of steady three-dimensional deep-water waves. *J. Fluid Mech.* **124**, 109–121.

MOLLO-CHRISTENSEN, E. 1981 Modulational stability of short-crested free surface waves. *Phys. Fluids* **24**, 775–776.

NAYFEH, A. H. 1971 Third harmonic resonance in the interaction of capillary and gravity waves. *J. Fluid Mech.* **48**, 385–395.

PENNEY, W. G. & PRICE, A. T. 1952 Some gravity wave problems in the motion of perfect liquids. Part 2: Finite periodic stationary gravity waves. *Phil. Trans. R. Soc. Lond.* A **244**, 251–284.

ROBERTS A. J. 1981 The behaviour of harmonic resonant steady solutions to a model differential equation. *Q. J. Mech. Appl. Maths* **34**, 287–310.

ROBERTS, A. J. 1982 Nonlinear buoyancy effects in fluids. Ph.D. thesis, University of Cambridge.

ROBERTS, A. J. & PEREGRINE, D. H. 1983 Notes on long-crested water waves. *J. Fluid Mech.* **135**, 323–335.

ROBERTS A. J. & SCHWARTZ, L. W. 1983 The calculation of nonlinear short-crested gravity waves. Submitted to *Phys. Fluids.*

ROTTMAN, J. W. 1982 Steep standing waves at a fluid interface. *J. Fluid Mech.* **124**, 283–306.

SCHWARTZ, L. W. 1974 Computer extension and analytic continuation of Stokes' expansion for gravity waves. *J. Fluid Mech.* **62**, 553–578.

SCHWARTZ, L. W. & WHITNEY, A. K. 1981 A semi-analytic solution for nonlinear standing waves in deep water. *J. Fluid Mech.* **107**, 147–171.

STOKES, G. G. 1880 Considerations relating to the greatest height of oscillatory waves which can be propagated without change of form. In *Mathematical and Physical Papers*, vol. 1, pp. 225–228. Cambridge University Press.

TADJBAKHSH, I. & KELLER, J. B. 1960 Standing surface waves of finite amplitude. *J. Fluid Mech.* **8**, 442–451.

WHITHAM, G. B. 1974 *Linear and Nonlinear Waves.* Wiley.